

LEGIBILITY NOTICE

A major purpose of the Technical Information Center is to provide the broadest dissemination possible of information contained in DOE's Research and Development Reports to business, industry, the academic community, and federal, state and local governments.

Although a small portion of this report is not reproducible, it is being made available to expedite the availability of information on the research discussed herein.

LA-UR--90-2294

DE90 015032

Received 11/28/91

AUG 06 1990

Los Alamos National Laboratory is operated by the University of California for the United States Department of Energy under contract W-7405-ENG-36

TITLE **THREE-DIMENSIONAL SIMULATIONS OF THE GENERATION OF
ONE ANGSTROM RADIATION BY A SELF-AMPLIFIED SPONTANEOUS
EMISSION FREE ELECTRON LASER**

AUTHOR(S) **J. C. Goldstein, C. J. Elliott, and M. J. Schmitt**

SUBMITTED TO **Proceedings of the Workshop on Prospects for a One Angstrom
Free Electron Laser
Brookhaven National Laboratory (BNL Report)
April 23 - 27, 1990**

DISCLAIMER

This report was prepared as an account of work sponsored by an agency of the United States Government. Neither the United States Government nor any agency thereof, nor any of their employees, makes any warranty, express or implied, or assumes any legal liability or responsibility for the accuracy, completeness, or usefulness of any information, apparatus, product, or process disclosed, or represents that its use would not infringe privately owned rights. Reference herein to any specific commercial product, process, or service by trade name, trademark, manufacturer, or otherwise does not necessarily constitute or imply its endorsement, recommendation, or favoring by the United States Government or any agency thereof. The views and opinions of authors expressed herein do not necessarily state or reflect those of the United States Government or any agency thereof.

By acceptance of this article, the publisher recognizes that the U.S. Government retains a nonexclusive, royalty-free license to publish or reproduce the published form of this contribution or to allow others to do so, for U.S. Government purposes.

The Los Alamos National Laboratory requests that the publisher identify this article as work performed under the auspices of the U.S. Department of Energy.

Los Alamos

Los Alamos National Laboratory
Los Alamos, New Mexico 87545

**Three-Dimensional Simulations of the Generation of One Angstrom Radiation
by a Self-Amplified Spontaneous Emission Free-Electron Laser***

J. C. Goldstein, C. J. Elliott, and M. J. Schmitt
Group X-1, MS E531
Los Alamos National Laboratory
Los Alamos, New Mexico 87545

Three-dimensional numerical simulations of the generation of one Angstrom X-rays by a free-electron laser operating in the self-amplified spontaneous emission mode have been performed. Using model electron beam and wiggler parameters, we have investigated the length of wiggler needed to just avoid bandwidth broadening effects associated with gain saturation, and we have also obtained requirements for wiggler field errors to avoid significant loss of performance.

I. Introduction

Self-amplified spontaneous emission (SASE) had been studied [1], [2], [3] as a possible method for the generation of extreme ultraviolet or soft x-ray radiation by free-electron lasers (FELs). In this scheme, no mirrors are needed in the light generation process, as they are for an FEL oscillator. This is a benefit, since highly reflective mirrors are not generally available at short wavelengths. However, the SASE scheme substantially increases the requirements on electron beam quality and wiggler length relative to those for a low-gain oscillator [4].

Requirements for SASE generation of one Angstrom radiation are extremely demanding. Rather than assess the possibility of achieving these requirements in general, we have used a set of electron beam and wiggler parameters proposed by Palmer and Gallardo [5] in their second letter of announcement of the BNL Workshop on Prospects for a One Angstrom Free-Electron Laser as model parameters. Using the 3-D FEL simulation code FELEX [6], [7] we have limited our ob-

*Work performed under the auspices of the U.S. Department of Energy and supported by Los Alamos Program Development funds.

jective in this study to a determination of the length of the wiggler that maximizes the power output but just avoids spectral broadening due to gain saturation effects. We have found that the appropriate wiggler contains over 1000 periods, and we have briefly studied the requirements on wiggler field errors with a trajectory correction scheme to avoid catastrophic loss of performance.

II. Model Parameters

The parameters in [5] assumed use of a helical wiggler magnet. Since the simulation code FELEX can handle only linearly polarized wigglers, we have adjusted two parameters in a way that leaves the critical FEL parameter, ρ , unchanged; for a linearly polarized wiggler, we have [3]

$$\rho = \left(\frac{G^2}{16\pi} r_e n_0 \left(\frac{a_w^2}{2} \right) \right)^{1/3} \left(\frac{\lambda_w^{2/3}}{\gamma} \right)$$

Here, $G = J_0(\xi) - J_1(\xi)$, where $\xi = a_w^2/(4 + 2a_w^2)$ and the J 's are Bessel functions. For a uniformly filled transverse phase-space distribution, the peak on-axis electron number density is given by $n_0 = 4k_\beta I/(3\epsilon c)$ [8], where I is the current, k_β is the betatron wave number (here equal to the reciprocal of the beta function [9]), ϵ , defined in [8], is four times the rms transverse emittance, e is the magnitude of the electron's charge, and c is the velocity of light. Other symbols used above are r_e , the classical radius of the electron; $\gamma = E/mc^2$ is the electron's relativistic factor; λ_w is the period of the wiggler magnet; and $a_w = e B_w \lambda_w/(2\pi mc^2)$ is the dimensionless vector potential where B_w is the peak wiggler magnetic field.

We choose B_w to make $0.5 a_w^2 = 1$, with $\lambda_w = 1$ cm. Using parameter values in [5], we find $n_0 = 2.923 \times 10^{17} \text{ cm}^{-3}$. We then define a new current $I' = I/G^2$ to make $G^2 n_0' = n_0$. These choices give a numerical value of $\rho = 1.09 \times 10^{-3}$, using 5 GeV for the electron beam energy. A summary of parameter values used in the simulations is given in Table 1. Note that the wiggler is assumed

to have curved-pole faces for two-plane focusing. Also, the betatron wavelength in [5] is far shorter (by a factor of 22) than that given by the “natural focusing” [8] of the wiggler, so some assumption about additional focusing has been made. The source of this focusing is unspecified, but might be produced by ion channels [10], [11]. An assumption of the numerical simulations is that this focusing is analogous to curved-pole-face focusing [12] in that the axial velocity is independent of the phase of an electron’s betatron oscillation. This is not true if external quadrupoles are used, and quadrupole focusing can lead to loss of gain due to dephasing of the electrons and light in a wiggler that is many betatron wavelengths long.

III. Simulations and Results

For an electron pulse length of 20 fs [5] and a wiggler 1000 periods long that radiates one Angstrom light, the electron pulse is about 60 slippage distances long. We have, therefore, neglected pulse effects in the simulations. We studied the dependence of the emitted power as a function of wiggler length via 3-D periodic boundary condition (pbc) [13] FELEX simulations. These calculations start from spontaneous emission due to shot noise in the electron current. For the wiggler length given in [5], 1020 periods, we calculated output powers in the range of 0.35-0.70 GW. The range is a result of calculations starting with different random number seeds. We repeated these calculations for longer wigglers and found that saturation effects just start at the end of a 1400 period wiggler. Figure (1) shows the radius of the electron beam in the wiggler. By “radius” we mean in this paper square root of $2 \times \text{rms}$ radius for both electron and optical beams; if the beam profiles were Gaussian, this would be the radius at the $1/e$ point. Figure (2) shows the optical beam radius inside the wiggler. The large initial growth occurs before guiding becomes dominant. The guided mode radius is about 12 μm , and the expansion at the end of the wiggler marks the onset of gain saturation. Figure (3) shows the onset of saturation at the end of the wiggler by tracking the change of the mean energy (dotted line) and the half widths at $1/e$ points (upper and lower solid lines). The mean energy drops and the energy spread increases, as the gain starts to saturate. These calculations yielded a power of about 8 GW and a fractional

spectral bandwidth of about 0.2% at the end of the wiggler. These values should be regarded as approximate because the difficulty of doing the simulations (note that $\epsilon \approx 10 \times$ optical wavelength) precluded many calculations.

For such long wigglers, one has to worry about the effects of wiggler field errors [14]. We have briefly investigated the constraints on field errors in the following way. We could not run FELEX in the pbc mode with field errors. Therefore, we defined an equivalent single-wavefront amplifier calculation: we used an initial input optical power that gave approximately the same output power (8 GW) and electron energy spread at the end of the wiggler as did the pbc calculation (which used multiple wavefronts and started from electron shot noise with no initial optical power). Figure (4) shows the evolution of the optical beam radius inside the wiggler for the single-wavefront calculation. The initial transient decays to the guided mode radius then starts to expand at the end of the wiggler as in Fig. (2). Figure (5) shows the onset of saturation from the electron beam mean energy and energy spread variations through the wiggler; it should be compared with Fig. (3). The gain of the equivalent single-wavefront amplifier calculation was about 6.5×10^3 , and the output power was about 8 GW.

We then introduced wiggler field errors [14] into the equivalent single-wavefront amplifier calculation and observed a reduction in performance. We have found the following results: The "matched" radius of the electron beam in the wiggler is about 6 μm . If the position of the beam can be sensed to $\pm 1 \mu\text{m}$, and if 10 steering stations are used along the length of the wiggler to bring the beam back to the axis, then wiggler field errors of about 0.01% can be tolerated. If the field errors are 0.02%, the performance drops by about a factor of two relative to the perfect wiggler case. If field errors are 0.01% but the beam position can be sensed to $\pm 2 \mu\text{m}$, the performance drops by somewhat more than a factor of two.

These are very stringent requirements. The requirement of 0.01% field errors is about a factor of 10 better than has been done in any wiggler yet constructed. The requirement of $\pm 1 \mu\text{m}$ beam position accuracy is also about one order of magnitude better than the present state of the art. One

should keep in mind that the state of the art for wiggler errors does not involve a 1400-period wiggler and that state-of-the-art position accuracy was not done for a 2.7-kA, 5-Gev, 20-fs electron beam. Hence, the required one-order-of-magnitude improvement may not adequately express the difficulty of achieving these goals.

IV. Summary and Conclusions.

We have studied some aspects of the generation of one-Angstrom radiation by numerical simulation methods. We used the electron beam and wiggler parameters of Case B in Ref. [5] as model parameters. We modified the wiggler field and peak current to keep the FEL parameter, ρ , in the simulations - which could be done only for a plane-polarized wiggler - equal to that in Ref. [5] (which considered using helical wigglers). Table 1 indicates parameter values used in the simulations.

Three-dimensional periodic boundary condition simulations that start from electron shot noise indicate that a 1400-period wiggler would produce a peak power of about 8 GW with a fractional bandwidth of about 2×10^{-3} centered at a wavelength of about one Angstrom. At this length, gain saturation effects are just beginning to be seen at the end of the wiggler.

We have briefly studied the effects of wiggler field errors on the performance of such an SASE device. We find that with 10 steering stations along the wiggler's length, the wiggler field errors must be held to 0.01% and the transverse position of the electron beam must be measurable to $\pm 1 \mu\text{m}$.

All of the separate requirements on the electron beam and the wiggler for this sort of one-Angstrom SASE FEL amplifier seem to substantially exceed achievements in existing devices. To achieve all of these requirements simultaneously, as is required for this device, would appear to require many years of development.

References

1. J. B. Murphy and C. Pellegrini, "Generation of High-Intensity Coherent Radiation in the Soft X-ray and Vacuum-Ultraviolet Region," *J. Opt. Soc. Am.* **113**, 530 (1985).
2. K. J. Kim, "Three-Dimensional Analysis of Coherent Amplification and Self-Amplified Spontaneous Emission in Free-Electron Lasers," *Phys. Rev. Lett.* **57**, pp. 1871-1874 (1986).
3. J. C. Goldstein, T. F. Wang, B. E. Newnam, and B. D. McVey, "A Single-Pass Free-Electron Laser for Soft X-rays with Wavelength Less Than or Equal to 10 Nanometers," in Proceedings of the IEEE Particle Accelerator Conference, E. R. Lindstrom and L. S. Taylor eds. (Institute of Electrical and Electronics Engineers, New York, 1987), pp. 202-204.
4. J. C. Goldstein, B. D. McVey, and C. J. Elliott, "Conceptual Design for a 50-nm FEL Oscillator and a 20 - 40-nm SASE Amplifier," *Nucl. Instr. and Meth. in Phys. Res.* **A272**, pp. 177-182 (1988).
5. R. B. Palmer and J. C. Gallardo, Example "B", letter dated February 9, 1990.
6. B. D. McVey, "Three-Dimensional Simulations of Free Electron Laser Physics," *Nucl. Instr. and Meth. in Phys. Res.* **A250**, pp. 449-455 (1986).
7. B. D. McVey, J. C. Goldstein, R. L. Tokar, C. J. Elliott, S. J. Gitomer, M. J. Schmitt, and L. E. Thode, "Numerical Simulations of Free Electron Laser Oscillators," *Nucl. Instr. and Meth. in Phys. Res.* **A285**, pp. 186-191 (1989).
8. J. C. Goldstein, B. D. McVey, and B. E. Newman, "Gain Physics of RF-Linac-Driven XUV Free-Electron Lasers," in Short Wavelength Coherent Radiation: Generation and Applications, AIP Conference Proceedings No. 147, D. T. Attwood and J. Bokor eds. (American Institute of Physics, New York, 1986), pp. 275-290.
9. C. Pellegrini, "Progress Toward a Soft X-ray FEL," *Nucl. Instr. and Met. in Phys. Res.* **A272**, pp. 364-367 (1988).
10. W. A. Barletta and A. M. Sessler, "Radiation from Fine, Intense, Self-Focused Beams at High Energy," Lawrence Livermore National Laboratory report number UCRL-98767, Rev. 1 (October 3, 1988).
11. D. H. Whittum, A. M. Sessler, and J. M. Dawson, "The Ion-Channel Laser," Lawrence Berkeley Laboratory report number LBL-28570 (January, 1990).
12. E. T. Scharlemann, "Wiggle Plane Focusing in Linear Wigglers," *J. Appl. Phys.* **58**, 2154 (1985).
13. W. B. Colson, "Chaotic Optical Modes in Free-Electron Lasers," in Free Electron Generators of Coherent Radiation, C. A. Brau, S. F. Jacobs, and M. O. Scully eds., *Proc. SPIE* **453**, pp. 290-296 (1984).
14. C. J. Elliott and B. D. McVey, "Analysis of Undulator Field Errors for XUV FELs," in Undulator Magnets for Synchrotrons and Free Electron Lasers, R. Bonifacio, L. Fonda, and C. Pellegrini, eds. (World Scientific Publishing Co., NJ, 1988), pp. 142-167.

Table 1. Parameter Values Used in the Simulations

Electron Beam

Peak current (A)	2702.703
$\gamma = E/mc^2$	9784.7358
$\Delta\gamma/\gamma$ (FW 1/e, %)	0.1
Normalized transverse emittance [87] (mm-mr)	0.8π
rms radius in wiggler (μm)	4.52

Wiggler

Wavelength (cm)	1.0
Peak field (T)	1.5132085
$k_\beta = 2\pi/\lambda_\beta$ (cm^{-1})	0.01

Optical

Resonance wavelength (Angstrom)	1.04448
---------------------------------	---------

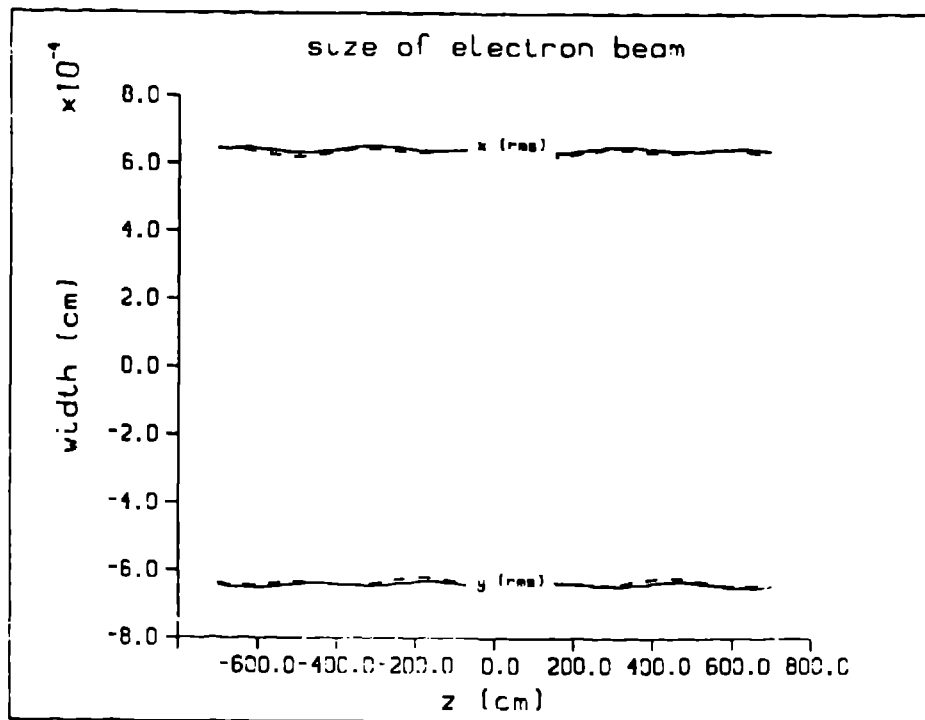


Figure 1: Radius of matched electron beam vs. longitudinal position inside the wiggler.

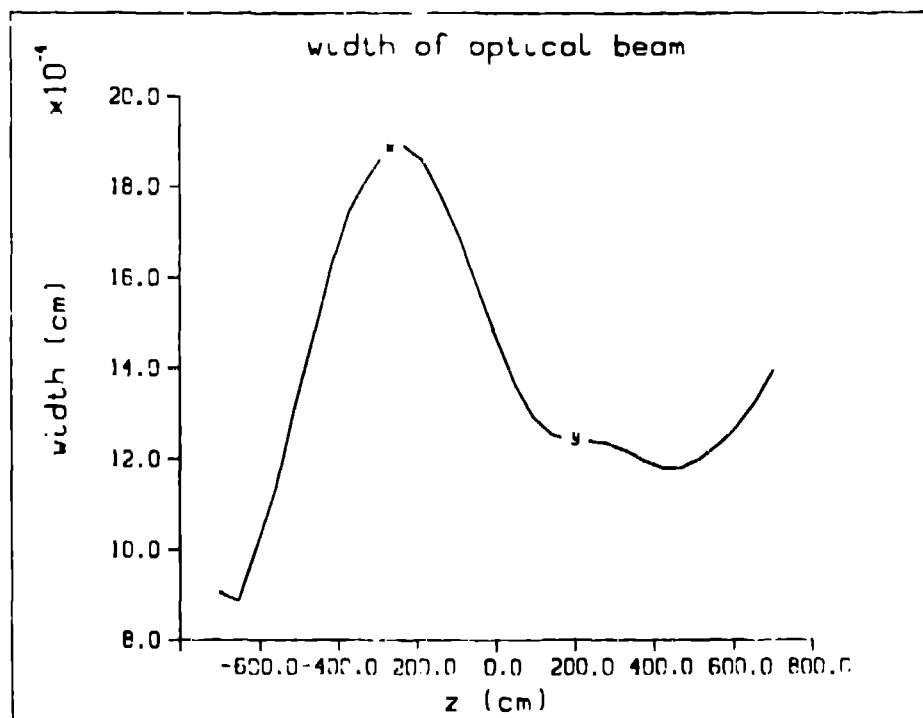


Figure 2: Radius of optical beam in periodic boundary condition simulation vs. longitudinal position along wiggler.

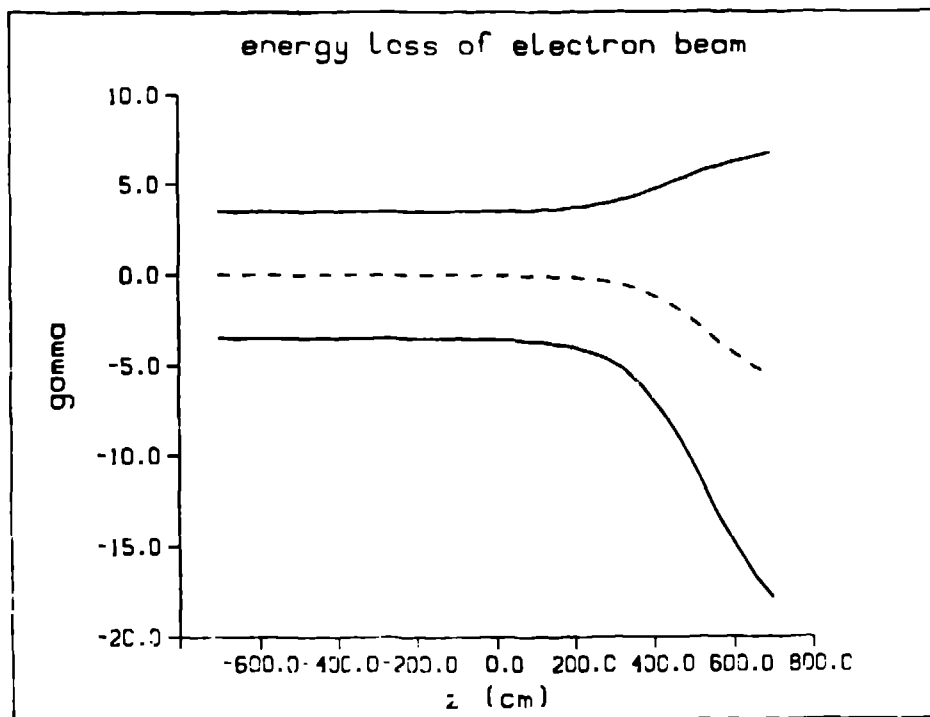


Figure 3: Mean energy (dotted) and energy spreads in pbc simulation vs. position along wiggler.

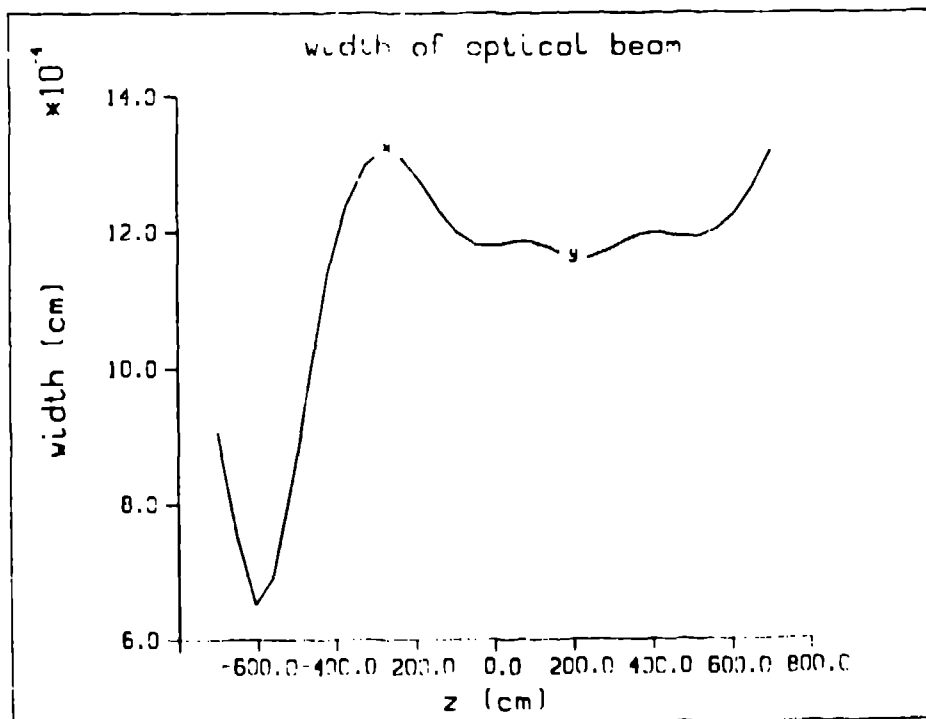


Figure 4: Radius of optical beam vs. position along wiggler for equivalent amplifier simulation.

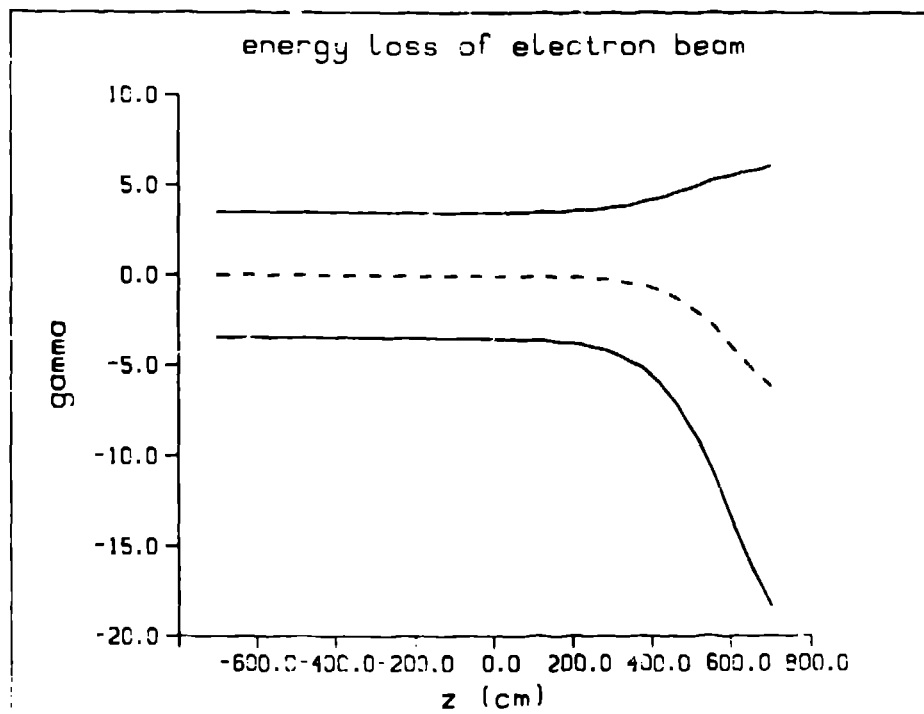


Figure 5: Mean energy (dotted) and energy spreads vs. position along wiggler for equivalent amplifier simulation.